Ultrafast dynamics in photoexcited valence-band states of Si studied by time- and angle-resolved photoemission spectroscopy of bulk direct transitions

Jun'ichi Kanasaki,[1] Hiroshi Tanimura,[2,*] Katsumi Tanimura,[1,2] Philip Ries,[3] Wolfgang Heckel,[3] Kerstin Biedermann,[3] and Thomas Fauster[3]

[1]*The Institute of Scientific and Industrial Research, Osaka University, Mihogaoka 8-1, Osaka 567-0047, Japan*
[2]*Research Center for Ultra-High Voltage Electron Microscopy, Osaka University, Mihogaoka 7-1, Osaka 567-0047, Japan*
[3]*Lehrstuhl für Festkörperphysik, Universität Erlangen-Nürnberg, Staudtstrasse 7, D-91058 Erlangen, Germany*

(Received 16 September 2017; revised manuscript received 25 November 2017; published 3 January 2018)

We identify direct-transition photoemission peaks from the bulk valence bands of Si in energy- and momentum-resolved photoemission from Si(111)-(7 × 7) using polarized 6-eV laser light. Time-resolved study of spectral line shapes of the peaks under interband excitation by 2-eV femtosecond-laser pulses shows the ultrafast transient spectral-width broadening and its recovery associated with a low-energy peak shift. The changes reveal the dynamics of screening effects by electron-hole plasma, hot-hole relaxation, and band renormalization in photoexcited Si, showing strong many-body effects in relaxation at excitation density less than 10^{18} cm^{-3}.

DOI: 10.1103/PhysRevB.97.035201

I. INTRODUCTION

Ultrafast dynamics of energetic carriers in semiconductors has been a strategic research field from both basic and applied science. Together with the accumulating knowledge obtained by extensive ultrafast optical spectroscopies [1–4], direct determination of transient hot-electron distributions in energy and momentum spaces by time- and angle-resolved photoemission spectroscopy [5–9] have made it possible to have deeper insight into the hot-electron dynamics in the conduction band (CB) of semiconductors. However, our knowledge of dynamics of photoexcited valence-band (VB) states in semiconductors has still been limited. Ultrafast dynamics of a specific VB state in semiconductors has been captured by infrared optical spectroscopy [10], but most knowledge is inferred indirectly from results of transport and optical measurements [11,12].

Time-resolved photoemission spectroscopy is capable of probing the dynamics of valence-band states [13]. In fact, ultrafast changes in populations at states below the Fermi level have been detected in Ru [14] and graphite [15]. In metal and semimetals, carrier-carrier (c-c) interaction is strong enough to establish a fast electronic quasithermalization, and the population changes in VB states may be characterized by an electronic temperature. In semiconductors, however, the screened Coulomb interaction is suppressed dramatically by the band gap on the order of 1 eV. How photoexcited VB states in semiconductors relax in ultrafast time scale is, therefore, still an important and relevant open question, since upon photoexcitation electrons and holes are likewise generated.

In ultraviolet photoelectron spectroscopy, photoelectrons with kinetic energies of a few tens of eV are analyzed [16], which correspond to the electron energy in solids near the minimum of the inelastic mean-free path of several angstroms [17]. This length scale is comparable to the depth of reconstructed surface layers, making the spectroscopy surface sensitive. One route to gain bulk sensitivity is to increase the photon energy to the hard x-ray range [18], which raises high demands on energy and angular resolution. The alternate route is to use probe light at photon energies less than 10 eV [19], where bulk sensitivity is enhanced strongly [17,19] and the parallel-momentum resolution is improved drastically.

Here we demonstrate that 6-eV polarized laser light can capture photoemission peaks of direct transitions from bulk valence bands of Si with (111) surface orientation reconstructed in the (7 × 7) structure. Time-, energy-, and angle-resolved measurements of bulk direct-transition peaks under interband optical excitation reveal features of ultrafast dynamics in screening effects and hot-hole relaxation in valence band of photoexcited Si.

II. EXPERIMENTAL

Boron-doped *p*-type Si(111) wafers were clamped with Ta sheets to the sample holder in an ultrahigh vacuum chamber ($< 3 \times 10^{-11}$ Torr). After appropriate thermal treatments, *in situ* scanning tunneling microscope observation showed (7 × 7) reconstructed structures with surface defects less than 0.05%. A laser system, consisting of a Ti-sapphire laser oscillator, a regenerative amplifier, and a tunable optical parametric amplifier, generated 65-fs pump laser pulses with pump-photon energies ($h\nu_{\mathrm{pump}}$) between 1.7 and 2.4 eV. The fluence of pump pulses was ranging from 13 to 76 μJ/cm^2. A part of the amplified fundamental output at 824 nm was used to generate the 80-fs third harmonics and 100-fs fourth harmonic pulses for probing photoemission. Pump and probe pulses, with a preset time delay (Δt), were aligned coaxially and focused on the sample surfaces at 45° to the axis of the electron analyzer. Measurements were made mostly at 90 K under the flat-band conditions for Si (111)-(7 × 7), established by pump-pulse excitation with a 250-kHz repetition rate [20]. A hemispherical

*Present address: Institute for Materials Research, Tohoku University, 2-1-1 Katahira, Aoba-ku, Sendai 980-8577, Japan.

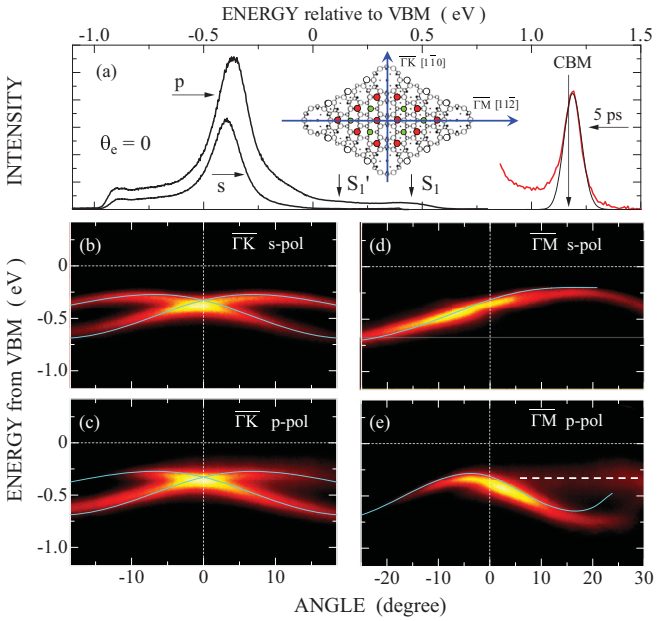

FIG. 1. (a) Photoemission spectra of normal emission probed by s- and p-polarized 6.02-eV light with the incident plane parallel to $\bar{\Gamma}\bar{K}$ ($[1\bar{1}0]$) direction. The red (dark gray) spectrum is that probed by 4.51-eV photons 5 ps after 2.21-eV pump-pulse excitation for the same specimen at 90 K. The thin solid curve is the fitted electron distribution function near the CBM at 90 K convolved with the 50-meV energy resolution. The inset shows the unit cell of (7×7) structure with directions along $\bar{\Gamma}\bar{M}$ and $\bar{\Gamma}\bar{K}$ of surface Brillouin zone. Red (dark gray) circles show adatoms, while green (gray) circles show rest atoms of (7×7) structure. (b)–(e) Two-dimensional $E(\theta)$ photoemission spectra for the Si(111)-(7×7) surface acquired along $[1\bar{1}0]$ directions with (b) s- and (c) p-polarized probe light, and those along the $[11\bar{2}]$ directions with (d) s- and (e) p-polarized light. Positive emission angles correspond to the increased angles between the surface normal and the optical path of incident probe lights over 45°. The light-blue (gray) curves are the results of theoretical analysis (see the text).

electron analyzer operated in an angle-resolved lens mode and a two-dimensional image-type detector served as the electron spectrometer. The energy resolution with fs-probe light was 50 meV, while angle resolution was ±0.5°.

III. RESULTS AND DISCUSSION

A. Photoemission peaks of direct transitions from bulk valence bands of Si

Figure 1(a) shows the normal-photoemission spectra probed by s- and p-polarized 6.02-eV light with the incident plane parallel to the $\bar{\Gamma}\bar{K}$ ($[1\bar{1}0]$) direction of the sample. The red curve in the figure shows the photoemission spectrum probed by 4.51-eV photons 5 ps after 2.21-eV pump-pulse excitation for the same specimen. This gives the photoemission peak from the thermalized electrons at the conduction band minimum (CBM). By applying the spectral-shape analysis as in Ref. [5], the kinetic energy of photoelectrons corresponding to the CBM is determined. Using this result, the initial-state energy E_i of photoemission probed by 6.02-eV photons is precisely referenced to the valence band maximum (VBM), since the flat-band condition is established. In the spectrum by s-polarized light, one intense peak at the initial-state energy $E_i = -0.40$ eV dominates. On the other hand, in the spectrum by p-polarized light, not only a similar peak at $E_i = -0.36$ eV, but also two other weak structures, labeled as S_1 and $S_1{\prime}$, are visible above the VBM at $E_i = +0.46$ and $+0.13$eV, respectively. The two peaks are from the S_1 and $S_1{\prime}$ surface-state bands of the (7×7) structure [21]. Here we focus our attention to the photoemission peaks with $E_i < 0$.

The dispersion of the photoemission peaks is shown in Figs. 1(b)–1(e) as a function of emission angle θ_e along $\bar{\Gamma}\bar{K}$ and $\bar{\Gamma}\bar{M}$ directions for s- and p-polarized probe light. Positive angles correspond to the increasing parallel momentum $k_\parallel$ from surface normal ($\theta_e = 0°$) toward the $[1\bar{1}0]$ or $[11\bar{2}]$ direction. In Figs. 1(b) and 1(c), the peak at $E_i = -0.36$ eV splits into two branches. The lower branch disperses downward, while the upper branch first disperses upward, reaches a maximum at $\theta_e = \pm 12°$, and then disperses downward. The dispersion in Fig. 1(b) is symmetric with respect to $\theta_e = 0°$, reflecting the mirror symmetry of the system with respect to the $(1\bar{1}0)$ crystallographic plane. In Fig. 1(c), the intensity of the upper branch is stronger at the positive-θ side than at negative θ. This comes from an accidental overlap of the surface-specific S_2 band photoionized selectively by the electric vector perpendicular to the surface. The same component is detected also in Fig. 1(e), where a dispersionless feature of the S_2 band (shown by a broken line) is more clearly visible.

Figures 1(d) and 1(e) present the photoemission images measured along the $\bar{\Gamma}\bar{M}$ direction using s- and p-polarized probe light. The electrons are emitted in a mirror plane. In Fig. 1(d), the dispersion shows a single intense peak with the highest energy of $E_i = -0.25$eV at $\theta_e = +15°$ to $[11\bar{2}]$. As the final state has to be even under reflection [22], odd (even) initial states are probed by s- (p-) polarized light. Note that the dispersion is not symmetric for $\pm k_\parallel$, although time-reversal symmetry requires $E(k_\parallel) = E(-k_\parallel)$. When photoemission proceeds via bulk bands as final states, the effect of group velocity $(v_g)_\perp$ perpendicular to the surface in the final state becomes crucial to describe the intensity as a function of $k_\parallel$. Depending on $(v_g)_\perp$, the electron can either propagate toward the surface for photoemission, or it can disappear into the bulk [23]. The sign of $(v_g)_\perp$ changes under reflection from $k_\parallel$ to $-k_\parallel$ and the electron in the bulk final state is emitted only in certain directions [24]. Therefore, the asymmetric dispersion is a consequence of photoemission from a bulk direct transition.

In order to quantify the qualitative arguments above, we employed the parametrized tight-binding scheme of Papaconstantopoulos using three-center integrals in a nonorthogonal basis [25]. For 6.02-eV probe light, only one final-state band with Λ_1 symmetry is relevant above the vacuum level $E_{\rm vac}$ (5.31 eV above VBM [6]), and a transition from the Λ_3 band leads to photoemission, as shown in Fig. 2(a). For each $k_\parallel$, the perpendicular momentum $k_\perp$ is scanned for direct transitions between Λ_3 valence and Λ_1 conduction bands at a photon energy of 6.02 eV. Only transitions with final-state energy above $E_{\rm vac}$ and a group velocity in the direction of the surface normal are kept. Resulting calculated dispersions are shown by the light-blue curves in Figs. 1(b)–1(e). The calculated results nicely fit the experimental data for both $\bar{\Gamma}\bar{K}$ and $\bar{\Gamma}\bar{M}$ directions. Along $\bar{\Gamma}\bar{M}$, some discrepancies are seen at large-θ region. The reason may be due to the incorrect description

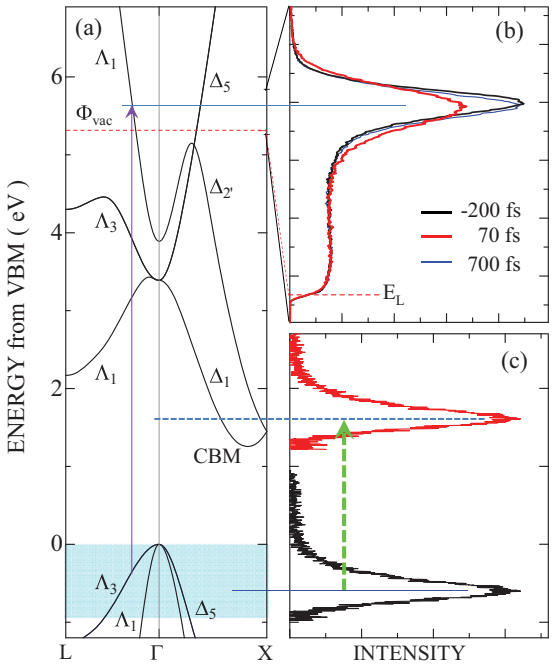

FIG. 2. (a) Electronic band structure of silicon along the L-Γ-X lines. The red (dark gray) dashed line indicates the vacuum level of Si(111)-(7 × 7); the ionization energy is 5.27 eV (Ref. [6]). The violet (gray) arrow illustrates a direct transition for 6.02-eV probe light. (b) Photoemission spectra probed by s-polarized 6.02-eV light at $\theta = 15°(E_i = -0.25$ eV) before pump-pulse excitation ($\Delta t = -200$ fs), solid, at $\Delta t = 70$ fs, red (dark gray), and at $\Delta t = 700$ fs, blue (gray). The broken line labeled E_L show the low-energy cutoff of the spectra, corresponding to the vacuum level at 5.31 eV. (c) Red (dark gray) curve shows the hot-electron distribution 70 fs after 2.21-eV photoexcitation probed by 4.51-eV light. The solid curve is the distribution function shifted downward by 2.21 eV, predicting hot-hole distribution under 2.21-eV excitation.

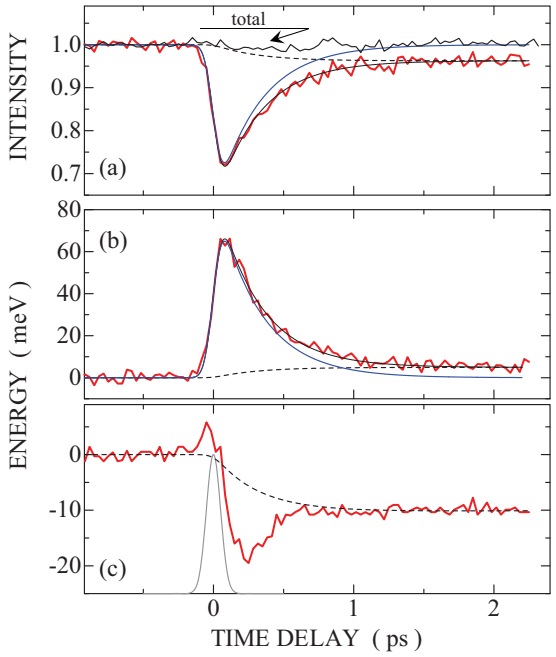

FIG. 3. (a) Temporal changes in the peak intensity measured at 5.93 eV in Fig. 2(b); (b) spectral width (full width at half maxima); and (c) peak energy of the photoemission spectra probed by s-polarized 6.02-eV light at $\theta = 15°(E_i = -0.25$eV). The thin solid curve labeled "total" in (a) is the photoemission intensities integrated with respect to energy from 5.6 to 6.10 eV in Fig. 2(b). The solid, broken, and blue (gray) curves are the results of rate-equation analysis.

of the band-structure calculations and/or the finite energy and momentum resolutions in experiment that broaden the peaks and flatten the dispersion curves. Thus the observed dispersive peaks are identified as direct transitions from the Λ_3 valence band to the Λ_1 conduction band in Si.

B. Ultrafast relaxation of photoexcited VB states in Si

As shown above, monitoring the bulk direct-transition peaks by 6-eV photons makes it possible to capture the changes in bulk electronic properties unambiguously with negligible contributions from surface-state photoemissions even for Si(111)-(7 × 7), one of the largest-scale reconstructed surfaces [26]. We use this technique to study relaxation of photoexcited VB states in Si. First, using 4.51-eV probe light, we determined the nascent hot-electron distribution photoinjected in the CB. The red curve in Fig. 2(c) displays the hot-electron distribution measured at 70 fs after 2.21-eV light pulses, showing a broad distribution with a peak at 0.7 eV above the CBM. The VB states participating in the optical transitions can be identified by shifting down the distribution by $h\nu_{pump}$ as shown by the solid curve. Hot holes are injected at the lowest energy of 0.9 eV below the VBM.

In Fig. 2(b), we show the photoemission spectrum 70 fs after excitation, probed by s-polarized 6.02-eV light at $\theta_e = 15°$ (corresponding $E_i = -0.25$ eV), and compare it with that before excitation. A drastic broadening of the width, associated with the reduced peak intensity, is evident with other underlying components almost unchanged. The width recovers to the original one at $\Delta t = 700$ fs as shown by the blue curve, but a finite low-energy shift of peak energy is clearly detected. The changes in spectral width ΔW, peak intensity I_p, and peak energy E_p as a function of Δt are summarized in Fig. 3. The changes are induced instantly during the overlap of pump and probe pulses, and they are relaxed mostly within $\Delta t < 1.0$ ps. However, small but finite changes persist at $\Delta t > 2$ps. In Fig. 4(a), the reduction of the peak intensity is plotted as a function of time delay up to 200 ps after excitation. It is evident that the rapid process shown in Fig. 3 follows a slow relaxation process lasting a few hundreds of ps. Therefore, we can conclude that the ultrafast process at $\Delta t < 1.0$ ps is the relaxation of photoinduced changes in VB state to establish a new metastable peak feature which lasts persistently.

Ultrafast changes in spectral features, together with a weak sublinear dependence of ΔW on the incident photon fluence Φ being described later, exclude any significant contributions of vacuum space-charge effect caused by the photoelectron clouds generated by nonlinear processes of pump pulses [27], as this effect induces spectral deformation on a time scale of several tens of ps before and after pump-probe overlap with strongly Φ-dependent magnitudes of deformation. Therefore

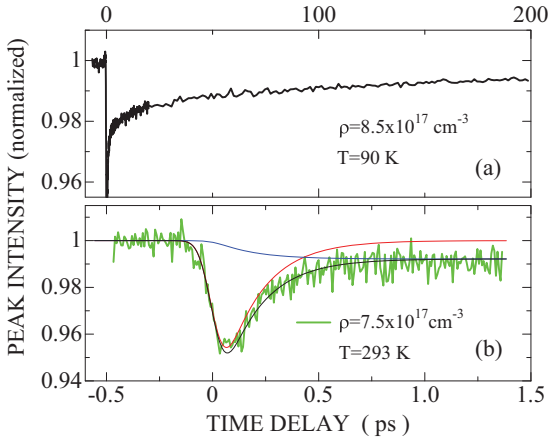

FIG. 4. (a) Temporal changes in the peak intensities of the bulk direct-transition peak probed by s-polarized 6.02-eV light at $\theta = 15^{\circ}(E_i = -0.25\text{eV})$ at extended time delay up to 200 ps measured at 90 K. (b) Temporal change in the peak intensities probed by s-polarized 6.02-eV light at $\theta = 15^{\circ}$ at 293 K. The red, blue, and black curves are the results of rate-equation analysis describing the decay of laser-induced changes, buildup of quasithermalized states with the same relaxation time, and sum of the two components, respectively. The relaxation time is 180 fs.

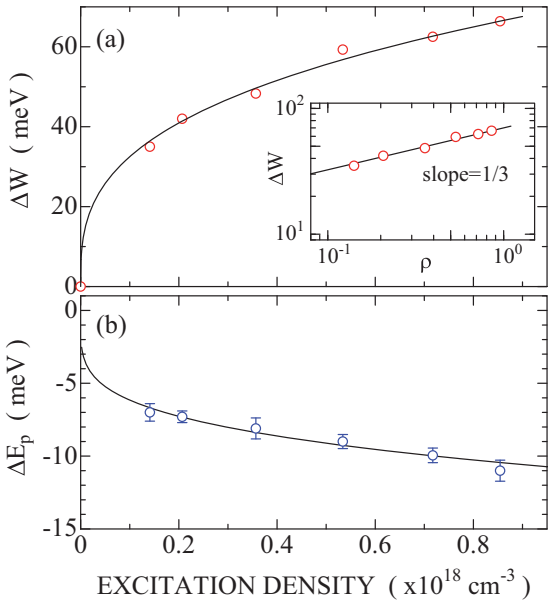

FIG. 5. (a) Dependence of the excitation-induced broadening ΔW of the spectral width of the bulk direct-transition peak on the excitation density ρ. The inset shows the plot at a logarithmic scale. The solid curves display the relation of $\Delta W = A\rho^{1/3}$, where A is constant. (b) Dependence of the peak-energy shift ΔE_p on ρ. The solid curve shows the density-dependent changes in the band-gap renormalization calculated by the method in Ref. [35] (a constant is multiplied to adjust the magnitude of ΔE_p).

the ultrafast changes shown in Fig. 3 reflect intrinsic dynamics of photoexcited VB states in Si.

The spectral width of a bulk direct-transition photoemission peak is determined by the lifetime broadenings at the final state (photoelectron) Γ_e and the initial state (photohole) Γ_h [28,29]. In view of the present energy range of photoexcitation, we can reasonably presume that Γ_e at the Λ_1 above E_{vac} is not affected directly. The relative contributions of Γ_e and Γ_h are also dependent on $(v_g)_\perp$ at the initial and final states. In the present case, probed by 6.02-eV photons, $(v_g)_\perp$ at the final state Λ_1 is 5 times larger than that at the initial state Λ_3. This makes the effects of Γ_h more pronounced. Therefore, ΔW results primarily from additional lifetime broadening of photohole by inelastic processes via c-c and/or electron-phonon (e-ph) interaction in the VB.

Because of the ultrafast changes within 200 fs associated with fast recovery in 1 ps after excitation, we can exclude possible incorporation of coherent LO phonons, if any, as the dephasing time (1.3 ps) of coherent LO phonons reported in Ref. [30] is much longer than the recovery time of the spectral broadening. Coherent acoustic phonons are excited at much longer time regime after photoexcitation as described in Ref. [31]. Therefore, electronic inelastic processes play dominant roles in laser-induced changes in spectral broadening. The c-c interaction in such a short time regime is governed by Coulomb quantum kinetics which includes buildup of plasma screening with a finite time [32]. In this regime, the c-c scattering rates depend on the carrier density ρ as $\rho^{1/3}$ for $\rho < 2 \times 10^{18}$ cm^{-3} in bulk semiconductors [3,33,34]. In order to examine this relationship, the maximum of ΔW around $\Delta t = 180$ fs is plotted as a function of ρ in Fig. 5(a). Here, ρ was evaluated using the equation $\rho = \Phi(1 - R)\alpha$, with incident photon fluence Φ of a fs-pump pulse, the reflectivity R, and the absorption coefficient α, with an estimated error of $\pm 10\%$., The results show clearly the relation $\Delta W = A\rho^{1/3}$, where A is a constant. Therefore, the initial broadening of spectral width is due to inelastic interaction with photoinjected holes having nonthermal distributions shown in Fig. 2(c). As the c-c interactions depend critically on the carrier distributions, the temporal change of ΔW at $\Delta t < 1$ps is representative of the relaxation of photoinjected hot holes to establish quasithermalized distribution near the VBM.

We simulate the quasithermalization rate using a rate-equation model with a single relaxation time τ. The best-fit results are shown by solid and broken curves in Fig. 3. The temporal changes of ΔW (and associated reduced I_P's) are well described with $\tau = 310$ fs. The magnitude of τ does not depend sensitively on ρ, partly because of weak dependence of $\rho^{1/3}$. On the other hand, we find that τ depends critically on temperature. In Fig. 4(b), the peak-intensity changes obtained by similar measurements at 293 K are shown, with the results of the rate-equation analysis. At 293 K, the time constant is reduced to 180 fs. Therefore, the e-ph interaction also plays important roles in relaxation process leading to hole quasithermalization.

Finally, we discuss another important feature, the peak-energy shift ΔE_p, captured by the analysis of the bulk direct-transition spectra. The peak-energy shift reveals electronic-structure changes upon interband electron-hole injection. After ultrafast transient changes, the new peak energy is established at 1 ps after excitation [Fig. 3(c)]. The present magnitude of ρ is higher than the Mott density (3.7×10^{17}cm^{-3}) at 90 K. Therefore, the peak-energy shift can be ascribed to the renormalization of valence-electronic system via significant exchange and

correlation interactions [35,36]. In Fig. 5(b), we show ΔE_p at $\Delta t = 1$ ps as a function of ρ. At $\rho = 8.4 \times 10^{17}\text{cm}^{-3}$ the peak-energy shift ΔE_p amounts to -12 meV, which is only 22% of band-gap renormalization ΔE_G predicted by the theory [35]. Nevertheless, the ρ dependence of ΔE_p is well described by the formula for ΔE_G in Ref. [35], indicating the same origin as ΔE_G. The negative shift of ΔE_p shows that the downward shift of the Λ_1 final state is larger than the opposite shift of the Λ_3 valence band at $\Delta t = 1$ps. The transient changes of ΔE_p shown in Fig. 3(c) may be representative of ultrafast dynamics of band renormalization induced by photoexcitation of Si. Although the band renormalization itself is a well-established concept, the ultrafast dynamics of many-body system leading to band renormalization in semiconductors is rather new. In fact, a theoretical study for the time-resolved band renormalization has been reported only recently [37]. Mechanisms that give rise to the ultrafast transient changes of ΔE_p are not clear at this moment. However, we could speculate that the dynamical change in ΔE_p is related to the temporal changes in screening effect, as it occurs at the timeframe when buildup of plasma screening evolves. This topic of band-renormalization dynamics has attracted strong attention to achieve dynamic tunability of the band gap and the electron dynamics for two-dimensional semiconductors [38].

IV. SUMMARY

We have identified, using 6-eV polarized laser light, photoemission peaks of direct transitions from bulk valence bands of Si with (111) surface orientation reconstructed in the (7×7) structure. Time- and angle-resolved photoemission spectroscopy of the direct bulk transitions under interband photoexcitation has revealed that even for $\rho < 10^{18}$ cm^{-3}, many-body effects of screening and band renormalization play important roles in the ultrafast relaxation processes in valence-band states in photoexcited Si. These features show strong contrast to those of hot-electron relaxation in the CB, where e-ph interaction is the dominant mechanism in ultrafast relaxation as demonstrated in Refs. [5] and [6].

ACKNOWLEDGMENT

This work was supported by JSPS KAKENHI Grant No. 24000006.

[1] J. Shah, *Ultrafast Spectroscopy of Semiconductors and Semiconductor Nanostructures*, 2nd ed. (Springer, Berlin, 1999).
[2] F. Rossi and T. Kuhn, Rev. Mod. Phys. **74**, 895 (2002).
[3] V. M. Axt and T. Kuhn, Rep. Prog. Phys. **67**, 433 (2004).
[4] R. P. Prasankumar, P. C. Upadhya, and A. J. Taylor, Phys. Status Solidi B **246**, 1973 (2009).
[5] T. Ichibayashi and K. Tanimura, Phys. Rev. Lett. **102**, 087403 (2009).
[6] T. Ichibayashi, S. Tanaka, J. Kanasaki, K. Tanimura, and Th. Fauster, Phys. Rev. B **84**, 235210 (2011).
[7] J. Kanasaki, H. Tanimura, and K. Tanimura, Phys. Rev. Lett. **113**, 237401 (2014).
[8] H. Tanimura, J. Kanasaki, and K. Tanimura, Phys. Rev. B **91**, 045201 (2015).
[9] H. Tanimura, J. Kanasaki, K. Tanimura, J. Sjakste, N. Vast, M. Calandra, and F. Mauri, Phys. Rev. B **93**, 161203(R) (2016).
[10] M. Woerner, W. Frey, M. T. Portella, C. Ludwig, T. Elsaesser, and W. Kaiser, Phys. Rev. B **49**, 17007 (1994).
[11] C. J. Stanton, D. W. Bailey, and K. Hess, Phys. Rev. Lett. **65**, 231 (1990).
[12] B. Fischer and K. R. Hofmann, Appl. Phys. Lett. **76**, 583 (2000).
[13] R. Haight, Surf. Sci. Rep. **21**, 275 (1995).
[14] M. Lisowski, P. A. Loukakos, U. Bovensiepen, J. Stähler, C. Gahl, and M. Wolf, Appl. Phys. A **78**, 165 (2004).
[15] A. Stange, C. Sohrt, L. X. Yang, G. Rohde, K. Janssen, P. Hein, L.-P. Oloff, K. Hanff, K. Rossnagel, and M. Bauer, Phys. Rev. B **92**, 184303 (2015).
[16] F. J. Himpsel, B. S. Meyerson, F. R. McFeely, J. F. Morar, A. Taleb-Ibrahimi, and J. A. Yarmoff, in *Photoemission and Absorption Spectroscopy of Solids and Interfaces with Synchrotron Radiation*, edited by M. Campagna and R. Rosei (North-Holland, Amsterdam, 1990), p. 203.
[17] K. Oura, V. G. Lifshits, A. A. Saranin, A. V. Zotov, and M. Katayama, *Surface Science: An Introduction* (Springer, Berlin, 2003).
[18] A. X. Gray, C. Papp, S. Ueda, B. Balke, Y. Yamashita, L. Plucinski, J. Minr, J. Braun, E. R. Ylvisaker, C. M. Schneider, W. E. Pickett, H. Ebert, K. Kobayashi, and C. S. Fadley, Nat. Mater. **10**, 759 (2011).
[19] T. Kiss, T. Shimojima, K. Ishizaka, A. Chainani, T. Togashi, T. Kanai, X.-Y. Wang, C.-T.Chen, S. Watanabe, and S. Shin, Rev. Sci. Instrum. **79**, 023106 (2008).
[20] J. E. Demuth, W. J. Thompson, N. J. DiNardo, and R. Imbihl, Phys. Rev. Lett. **56**, 1408 (1986).
[21] T. Ichibayashi and K. Tanimura, Phys. Rev. B **75**, 235327 (2007).
[22] W. Eberhardt and F. J. Himpsel, Phys. Rev. B **21**, 5572 (1980).
[23] W. Schattke, E. E. Krasovskii, R. Díez Muiño, and P. M. Echenique, Phys. Rev. B **78**, 155314 (2008).
[24] K. Biedermann, S. Regensburger, Th. Fauster, F. J. Himpsel, and S. C. Erwin, Phys. Rev. B **85**, 245413 (2012).
[25] D. A. Papaconstantopoulos, *Handbook of the Band Structure of Elemental Solids* (Plenum, New York, 1986).
[26] W. Mönch, *Semiconductor Surfaces and Interfaces* (Springer, Berlin, 1995).
[27] L.-P. Oloff, K. Hanff, A. Stange, G. Rohde, F. Diekmann, M. Bauer, and K. Rossnagel, J. Appl. Phys. **119**, 225106 (2016).
[28] N. V. Smith, P. Thiry, and Y. Petroff, Phys. Rev. B **47**, 15476 (1993).
[29] P. M. Echenique, R. Berndt, E. V. Chulkov, Th. Fauster, A. Goldmann, and U. Höfer, Surf. Sci. Rep. **52**, 219 (2004).
[30] M. Hase, M. Kitajima, A. M. Constantinescu, and H. Petek, Nature (London) **426**, 51 (2003).
[31] K. Ishioka, A. Rustagi, U. Höfer, H. Petek, and C. J. Stanton, Phys. Rev. B **95**, 035205 (2017).
[32] R. Huber, F. Tauser, A. Brodschelm, M. Bichler, G. Abstreiter, and A. Leitenstorfer, Nature (London) **414**, 286 (2001).
[33] P. C. Becker, H. L. Fragnito, C. H. B. Cruz, R. L. Fork, J. E. Cunningham, J. E. Henry, and C. V. Shank, Phys. Rev. Lett. **61**, 1647 (1988).

[34] W. A. Hügel, M. F. Heinrich, M. Wegener, Q. T. Vu, L. Bányai, and H. Haug, Phys. Rev. Lett. **83**, 3313 (1999).

[35] P. Vashishta and R. K. Kalia, Phys. Rev. B **25**, 6492 (1982).

[36] T. J. Inagaki and M. Aihara, Phys. Rev. B **65**, 205204 (2002).

[37] D. Sangalli, S. D. Conte, C. Manzoni, G. Cerullo, and A. Marini, Phys. Rev. B **93**, 195205 (2016).

[38] S. Ulstrup, A. G. Cabo, J. A. Miwa, J. M. Riley, S. S. Grønborg, J. C. Johannsen, C. Cacho, O. Alexander, R. T. Chapman, E. Springate, M. Bianchi, M. Dendzik, J. V. Lauritsen, P. D. C. King, and P. Hofmann, ACS Nano **10**, 6315 (2016).